

# EXTRAPOLATION METHODS FOR IMPROVING MR PERFUSION MEASUREMENTS

M Ethan MacDonald<sup>1,2,5</sup>, Richard Frayne<sup>1-5</sup>, and Michael R Smith<sup>1,2,3</sup>  
<sup>1</sup>Electrical and Computer Engineering, <sup>2</sup>Biomedical Engineering,  
<sup>3</sup>Radiology, <sup>4</sup>Clinical Neurosciences, University of Calgary,  
and <sup>5</sup>Seaman Family MR Research Centre, Foothills Medical Centre

## INTRODUCTION

The quantification of cerebral blood flow (CBF) in patients suffering from ischemic stroke will likely become a key clinical tool for assessing their prognosis. By its very definition, ischemic stroke represents a reduction of blood flow (ischemia) to a region of brain tissue, most commonly due to a blocked vessel. Magnetic resonance (MR) perfusion imaging can provide estimates of CBF by monitoring the passage of a gadolinium-based contrast agent as it travels through the cerebral vascular system over time.[1,2] During contrast passage, images are gathered every 1 s to 2 s over a period of 60 s to 90 s. From these images a signal intensity time series can be constructed for each image voxel. Measured signal intensity decreases as the contrast agent passes with a logarithmic relationship relating concentration of the tracer ( $C(t)$ ) and intensity ( $S(t)$ ),

$$C(t) \propto -\ln\left(\frac{S(t)}{S_0}\right), \quad (1)$$

where  $S_0$  is the initial MR signal intensity before contrast agent arrival. Eq (1) represents the fundamental relationship that relates signal intensity in a voxel to concentration of contrast agent.

The relationship between concentration and CBF is well established in MR perfusion. If an arterial concentration function,  $C_a(t)$ , is selected from an artery supplying blood to the brain, then CBF can be calculated in a tissue volume-of-interest (VOI),  $C_{VOI}(t)$ ,

$$C_{VOI}(t) = CBF * R(t) \otimes C_a(t), \quad (2)$$

where  $R(t)$  represents the tissue residue function or the normalized system response that has a peak of 1.[1-3] From Eq (2), CBF can be estimated by performing deconvolution. Traditionally this has been performed in the time domain using the matrix formulation,

$$C_{VOI} = C_a \mathbf{R}' \quad (3)$$

and,

$$CBF = \max\{\mathbf{R}'\}, \quad (4)$$

where  $\mathbf{R}' = CBF * R$  and the continuous time function has been discretised, such that;

$$\begin{bmatrix} C_{VOI}[0] \\ C_{VOI}[1] \\ \dots \\ C_{VOI}[N-1] \end{bmatrix} = \begin{bmatrix} C_a[0] & C_a[N-1] & \dots & C_a[1] \\ C_a[1] & C_a[0] & \dots & C_a[2] \\ \dots & \dots & \dots & \dots \\ C_a[N-1] & C_a[N-2] & \dots & C_a[0] \end{bmatrix} \begin{bmatrix} R'[0] \\ R'[1] \\ \dots \\ R'[N-1] \end{bmatrix}. \quad (4)$$

The maximum of the  $\mathbf{R}'$  vector is the CBF estimate. This process requires inversion of  $C_a$ , which in the presence of noise is a process that can be unstable. Singular value decomposition (SVD) is often used to stabilize the inversion process. In SVD the matrix  $C_a$  is divided into three separate matrices,

$$C_a = \mathbf{U} \mathbf{W} \mathbf{V}^T. \quad (5)$$

After decomposition, the diagonal matrix  $\mathbf{W}$  contains the normalized Eigen values of  $C_a$ . The superscript T denotes transpose. The inverse of  $C_a$  can be found by,

$$C_a^{-1} = \mathbf{V} \left[ \text{diag} \left( \frac{1}{\omega_i} \right) \right] \mathbf{U}^T. \quad (6)$$

To ensure stability, Eigen values ( $\omega_i$ ) below a certain threshold are removed. In practice the threshold value is  $P_{SVD} = 0.2$ , or 20% of the largest Eigen value.[4]

Alternatively, deconvolution can be performed by division in the frequency domain,

$$R'(t) = \mathfrak{F}^{-1} \left\{ \frac{C_{VOI}(f)}{C_a(f)} \right\} \quad (7)$$

and,

$$CBF = \max\{R'(t)\}, \quad (8)$$

where  $C_a(f)$  and  $C_{VOI}(f)$  are the Fourier transforms (FT) of  $C_a(t)$  and  $C_{VOI}(t)$ , respectively. Fourier deconvolution is itself not stable and requires low-pass filtering to remove instabilities often found at higher frequencies.

Salluzzi *et al.* [5] demonstrated the similarities between the SVD and FT deconvolution approaches; most notably elucidating the relationship between  $P_{SVD}$  and the low-pass filter applied to the frequency domain data,

$$w_f = \begin{cases} 1 & |C_a(f)| < P_{SVD} * |C_a(f)|_{\max} \\ 0 & \dots \end{cases} \quad (9)$$

This expression agrees with the notion of relating Eigen values asymptotically to Fourier transform coefficients.[6]

## THEORY

The function  $C_a$  may be approximated as a normalized gamma-variate function,

$$C_a(t) \cong \begin{cases} \frac{C_{\max} (t-T_A)^\alpha e^{-(t-T_A)/\beta}}{(\alpha\beta)^\alpha e^{-\alpha}} & t > T_A, \\ 0 & \dots \end{cases}, \quad (10)$$

where  $\alpha$  and  $\beta$  are constants, generally set to 3 and 1.5 s, respectively,[5]  $T_A$  represents the arrival time of the contrast agent, and  $C_{\max}$  is the maximum value of the concentration function. Most commonly the residue function is approximated as an exponential decay,[4,5]

$$R(t) \cong e^{-(t-ATD)/MTT}, \quad (11)$$

with MTT being the mean transit time and ATD, the arterial-tissue delay. MTT is the average time for the contrast agent to pass through the tissue. To find  $C_{VOI}(t)$ , we performed the numeric convolution of Eq (2).

Noise in MR applications has a Gaussian distribution when added separately to the in-phase and quadrature signals. The non-linearity of Eq (1) results in non-Gaussian noise on concentration signals,[3] as the logarithmic function makes the noise variance dependant on the amplitude of the concentration function. This non-linear noise behavior, combined with the deconvolution creates instabilities in the residue function (Fig 1).

The need for filtering or thresholding to regain stability should be clear from Fig 1. However, this filter also removes high-frequency components of  $R'(t)$ , resulting in a misrepresentation of the  $R'(t)$  peak, and thus introducing model-based errors into CBF. This error is relative to the width of  $R(t)$ : as the signal becomes shorter in time it becomes broader in frequency, leading the filter to remove more of the signal. This effect is dependant on the amount of filtering or threshold value (Fig 2). As  $P_{SVD}$  increases, more of the corresponding signal is removed, resulting in more model-based error.

*By reintroducing or recovering this high-frequency information through simple linear extrapolation algorithms, we expect that a better estimate of CBF can be obtained.*

## METHODS

### Simulations

A simple linear approach was used for extrapolation. More sophisticated techniques, such as the autoregressive moving average (ARMA)[7] were considered, but were found to be not well suited for this application, principally due to the small number of points available and the large distance that needed to be extrapolated. With simple linear extrapolation, the signal is drawn from the last non-filtered point down to a value of zero at some distance ( $\ell$ ) away. This process is best illustrated in the frequency domain and must be done for both the real and imaginary components, as depicted in Fig 3.

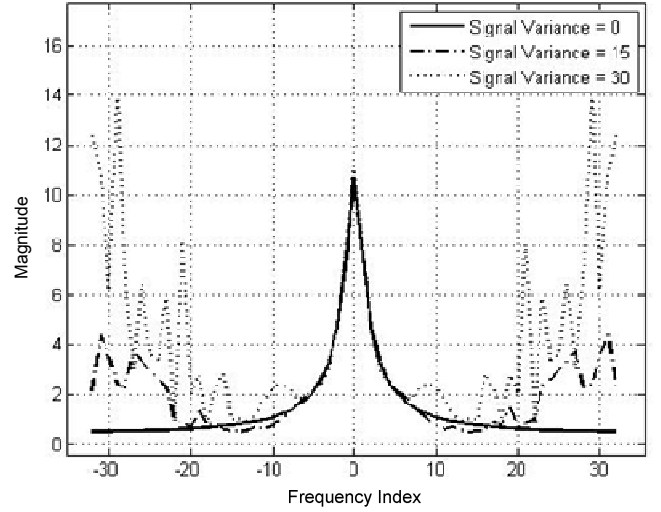


Figure 1: The magnitude of the residue function frequency spectrum is depicted. The signal is obtained by deconvolving the arterial and volume-of-interest functions (MTT and ATD of 8 s and 0.01 s, respectively). Gaussian noise was added to the MR signal intensity with variances of 0, 15 and 30 on an initial signal intensity of  $S_0 = 1000$ , ( $SNR = S_0/\sigma_N$ ). High-frequency noise effects increased with increasing noise variance of the MR signal intensity.

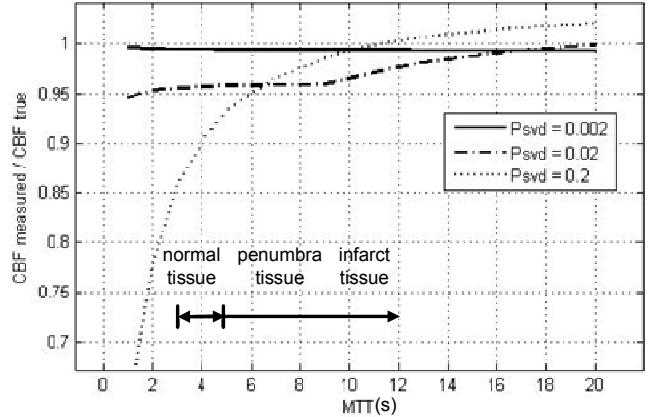


Figure 2: With increasing  $P_{SVD}$  more high frequency signals are removed from  $R'(t)$ . This in turn causes an expected error in the peak of the  $R'(t)$ , which is dependent on the width of the signal in time: As MTT decreases, the signal becomes broader in the frequency domain and more signal energy is removed, thus resulting in more error. The MTT ranges indicate normal, penumbral (potentially recoverable with proper treatment) and infarcted (unlikely to recover) tissues.

Determination of the distance over which extrapolation should be performed initially seemed problematic. Intuitively, as MTT becomes larger,  $R'(t)$  becomes narrower and taller in the frequency domain. Thus for longer MTT extrapolation over a shorter distance should be expected. Closer examination and manipulation of Eq. (11) suggested:

$$R(f) \cong \frac{e^{-j2\pi f ATD}}{\frac{1}{MTT} + j2\pi f}, \quad (12)$$

where,

$$R(f) \cong MTT ; f = 0. \quad (13)$$

This manipulation suggested that the height of  $R(f)$  at  $f = 0$  can estimate MTT.

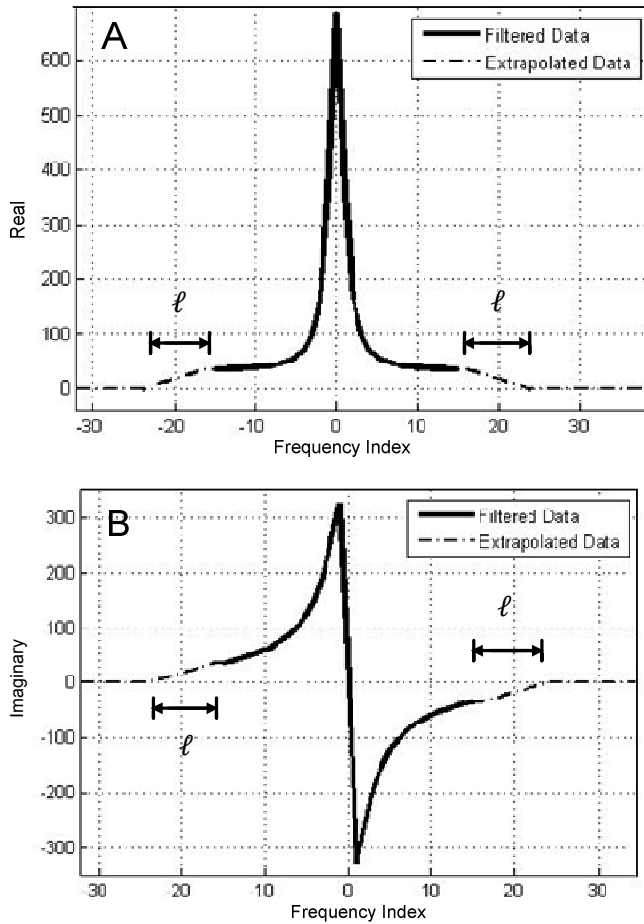


Figure 3: Real (A) and imaginary (B) components, of the residue function in the frequency domain. The filtered data corresponds to the data that is left after the high frequencies have been removed. The extrapolated data represents the data that has been estimated linearly from the last unfiltered point to zero at a distance  $\ell$  away.

Letting,

$$\ell = \frac{C}{MTT}, \quad (14)$$

where  $C$  is an arbitrary constant. Different responses for extrapolation can be obtained by changing the value of  $C$ . We examined  $20 \text{ s} < C < 60 \text{ s}$ .

#### Patient Data

MR perfusion image data sets were analyzed. Arterial input functions were selected from individual pixels based on signal characteristics and anatomical location. The simple extrapolation method was used to recover SVD-thresholded data. As per convention, the results were cross-calibrated so that normal white matter had a CBF of  $22 \text{ ml} / 100 \text{ g} / \text{min}$ .

Throughout this study, MATLAB was used, for all simulation and image reconstructions. In addition, testing software, MUnit, was used to improve the robustness of algorithms. This development platform allowed for speedy, robust prototyping.

## RESULTS

#### Simulations

The CBF measured over CBF true versus MTT plots were obtained using a noiseless simulation to determine an appropriate extrapolation constant (Fig 4).  $C$  was chosen to be 60, as this value caused CBF to behave independ-

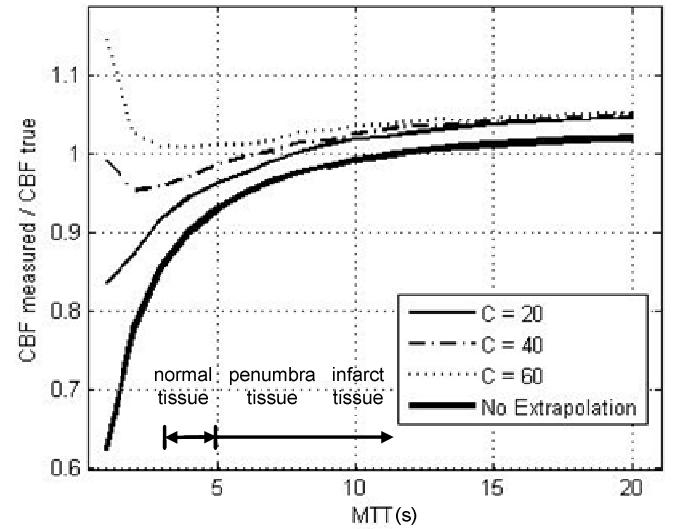


Figure 4: For  $P_{SVD} = 0.2$ ; the measured/true CBF ratio is plotted against MTT, for signals with no extrapolation and with extrapolation. Extrapolation was performed for  $C = 20 \text{ s}$ ,  $40 \text{ s}$  and  $60 \text{ s}$ ; these correspond to extrapolation distances  $\ell = C/MTT$  as per Eq (14).

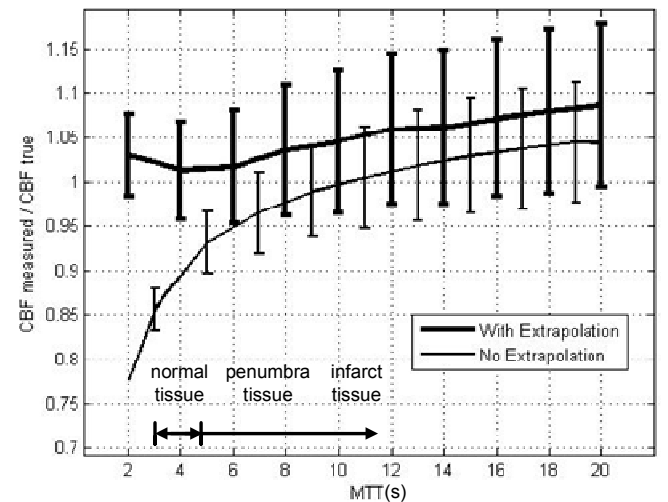


Figure 5:  $C = 60 \text{ s}$  was used for extrapolation in a Monte Carlo simulation and compared with no extrapolation, Gaussian noise has been added to MR signal intensity ( $S_0 = 1000$ ,  $\sigma_N^2 = 20$ ). The error bars represent 2 standard deviations.

ently of MTT over the practical range of normal and infarcted tissues ( $3 \text{ s} < MTT < 20 \text{ s}$ ). Monte Carlo simulations, with noise, were undertaken to ensure the algorithm was stable (Fig 5). The improved accuracy (CBF ratio  $\sim 1.0$ ) was demonstrated. As expected the extrapolated measures were less precise.

#### Patient Data

A patient data was selected with a moderate stroke and processed (Fig 6). The time-to-peak (TTP) map showed a blood flow abnormality (Fig 6a, arrow). Deconvolution was performed using both the filtered and simple extrapolation methods. In both cases the same pixels were chosen for the arterial function and for cross-calibration. Qualitatively, the extrapolation technique (Fig 6c) better depicts the blood flow abnormality identified in the TTP map. The difference image (Fig 6d) showed us the numerical difference between the two techniques, it should be noted that the difference map almost uniformly removes image intensity. This can be thought of as an

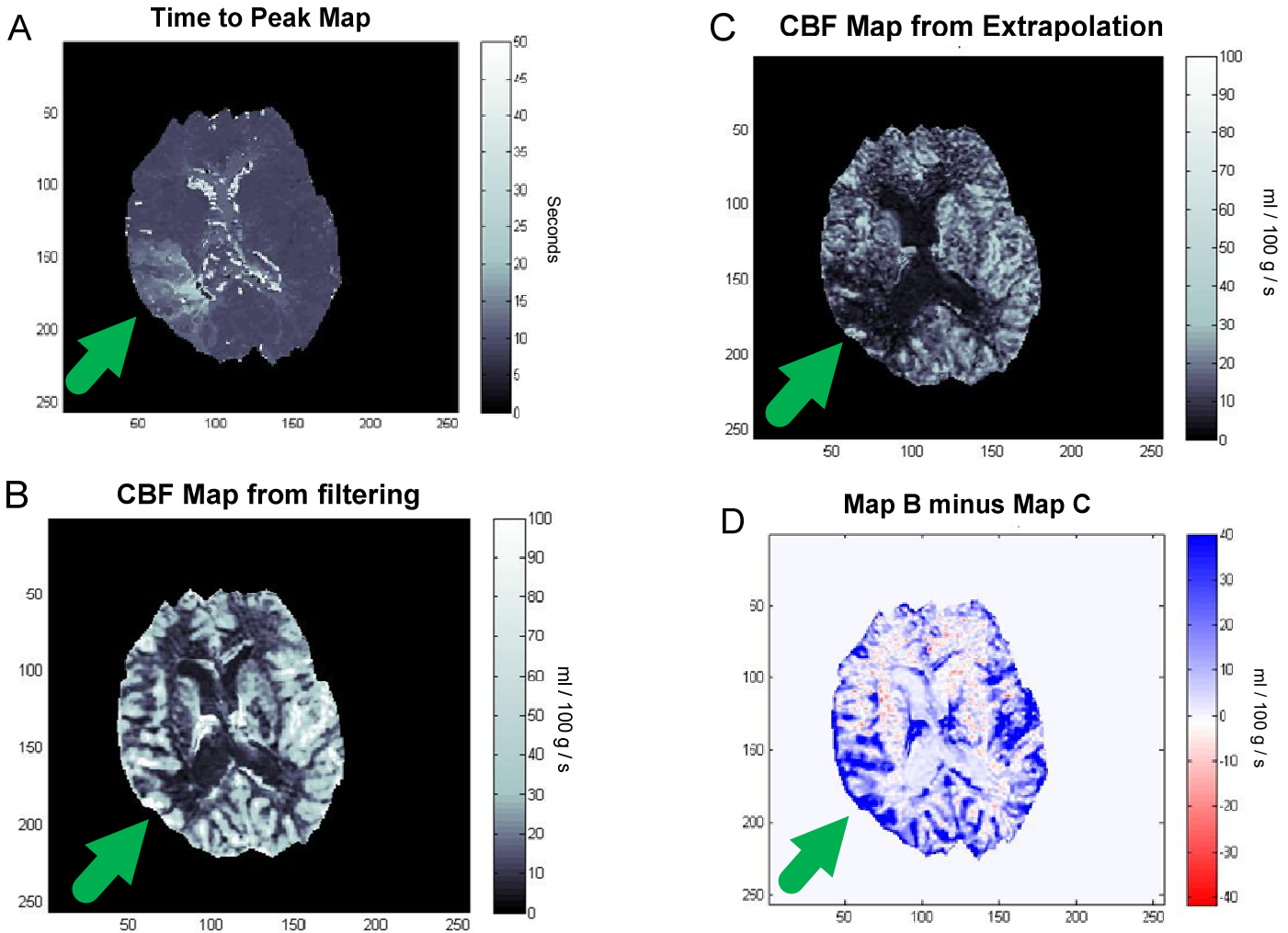


Figure 6: Image (A) represents time-to-peak (TTP) map of the concentration of tracer showing an area with delayed filling (arrow). (B) is a CBF map obtained by performing a Fourier-domain deconvolution, filtering and cross calibrating. (C) is a CBF map obtained by Fourier-domain deconvolution, filtering, extrapolation (with  $\mathcal{C} = 60$  s), and then cross calibrating. (D) is the difference map between (B) and (C). The stroke region (arrow) is better defined in C than in B.

improvement in contrast, under the definition,

$$\text{Contrast} = \frac{|I_{\text{Stroke}} - I_{\text{Normal}}|}{I_{\text{Stroke}} + I_{\text{Normal}}}. \quad (15)$$

The difference remains the same, however the amplitudes are decreased.

### CONCLUSION

While it is intuitive to think that information representing blood flow can be obtained from the passage of contrast agent; in practice the best way to process this information is not obvious. Here, we have presented a model-specific data extrapolation technique and compared results with conventional approaches. From Fig 6c, we see an increase of noise in the image. This agrees with simulation results as there is an increase of noise in healthy tissue. Further investigation of patient data and refinements in processing and modeling, such as preservation of continuity,[8] will no doubt lead to improvements in estimates. More reliable information about blood flow results in better assessment of penumbral and infarcted tissue.

### ACKNOWLEDGEMENTS

We thank NSERC and CIHR for financial support, as well as M. Salluzzi, J.C. Koisor and J. Qiao.

### REFERENCES

- [1] L Østergaard, R Weisskoff, DA Chesler, C Gyldensted, BR Rosen, *High Resolution Measurement of Cerebral Blood Flow using Intravascular Tracer Bolus Passages. Part I: Mathematical Approach and Statistical Analysis*. Magnetic Resonance in Medicine, 1996.36: p.715-725.
- [2] MR Smith, H Lu, R Frayne. *Correcting Systematic Biases in Quantitative Cerebral Blood Flow Estimates From Dynamic Susceptibility Contrast MR Perfusion Studies*. in *Proceedings of the MEDSIP 2nd International Conference on Advances in Medical and Image Processing*. 2004. Malta, G.C.
- [3] MR Smith, H Lu, R Frayne, *Signal-to-Noise Ratio Effects in Quantitative Cerebral Perfusion Using Dynamic Susceptibility Contrast Agents*. Magnetic Resonance in Medicine, 2003. 49: p. 122-128.
- [4] K Murase, M Shinohara, Y Yamazaki, *Accuracy of deconvolution analysis based on singularvalue decomposition for quantification of cerebral blood flow using dynamic susceptibility contrast-enhanced magnetic resonance imaging*. Physics in Medicine and Biology, 2001(46): p. 3147-3159.
- [5] M Salluzzi, R Frayne. M R Smith., *An alternative viewpoint of the similarities and differences of SVD and FT deconvolution algorithms used for quantitative MR perfusion studies*. Magnetic Resonance Imaging, 2005(23): p. 481-492.
- [6] S Kay, *Fundamentals of Statistical Signal Processing: Detection Theory*. 1998: Prentice Hall.
- [7] H Lu, M Smith, R Frayne. *Quantitative MR Cerebral Blood Flow Using ARMA-based Deconvolution: Preliminary Results*. in *IEEE Canadian Conference on Electrical and Commter Engineering*. 2002: IEEE.
- [8] FJ Harris, *On the Use of Windows for Harmonic Analysis with the Discrete Fourier Transform*. Proceedings of the IEEE, 1978. 66(1): p. 51-83.